LETTER

doi:10.1038/nature10652

A gas cloud on its way towards the supermassive black hole at the Galactic Centre

S. Gillessen[1], R. Genzel[1,2], T. K. Fritz[1], E. Quataert[3], C. Alig[4], A. Burkert[4,1], J. Cuadra[5], F. Eisenhauer[1], O. Pfuhl[1], K. Dodds-Eden[1], C. F. Gammie[6] & T. Ott[1]

Measurements of stellar orbits[1–3] provide compelling evidence[4,5] that the compact radio source Sagittarius A* at the Galactic Centre is a black hole four million times the mass of the Sun. With the exception of modest X-ray and infrared flares[6,7], Sgr A* is surprisingly faint, suggesting that the accretion rate and radiation efficiency near the event horizon are currently very low[3,8]. Here we report the presence of a dense gas cloud approximately three times the mass of Earth that is falling into the accretion zone of Sgr A*. Our observations tightly constrain the cloud's orbit to be highly eccentric, with an innermost radius of approach of only ~3,100 times the event horizon that will be reached in 2013. Over the past three years the cloud has begun to disrupt, probably mainly through tidal shearing arising from the black hole's gravitational force. The cloud's dynamic evolution and radiation in the next few years will probe the properties of the accretion flow and the feeding processes of the supermassive black hole. The kilo-electronvolt X-ray emission of Sgr A* may brighten significantly when the cloud reaches pericentre. There may also be a giant radiation flare several years from now if the cloud breaks up and its fragments feed gas into the central accretion zone.

As part of our NACO[9] and SINFONI[10,11] Very Large Telescope (VLT) observation programmes studying the stellar orbits around the Galactic Centre supermassive black hole, Sgr A*, we have discovered an object moving at about 1,700 km s^{-1} along a trajectory almost straight towards Sgr A* (Fig. 1). The object has a remarkably low temperature (about 550 K; Supplementary Fig. 2) and a luminosity about five times that of the Sun, unlike any star we have so far seen near Sgr A*. It is also seen in the spectroscopic data as a redshifted emission component in the Brγ and Brδ hydrogen lines, and the 2.058 μm He I lines, with the same proper motion as the L′-band object. Its three-dimensional velocity increased from 1,200 km s^{-1} in 2004 to 2,350 km s^{-1} in 2011. The Brγ emission is elongated along its direction of motion with a spatially resolved velocity gradient (Fig. 2). Together, these findings show that the object is a dusty, ionized gas cloud.

The extinction of the ionized gas is typical for the central parsec (Supplementary Information section 1) and its intrinsic Brγ luminosity is 1.66 ($\pm$0.25) $\times$ 10^{-3} times that of the Sun. For case B recombination the implied electron density is $n_c = 2.6 \times 10^5 f_V^{-1/2} R_c^{-3/2} T_e^{0.54}$ cm^{-3}, for an effective cloud radius of $R_c \approx 15$ milli-arcseconds (mas), volume filling factor f_V ($\leq$1) and an assumed electron temperature T_e in units of 10^4 K, a value typical for the temperatures measured in the central parsec[12]. The cloud mass is $M_c = 1.7 \times 10^{28} f_V^{1/2} R_c^{3/2} T_e^{0.54}$ g or about $3 f_V^{1/2}$ Earth masses. It may plausibly be photo-ionized by the ultraviolet radiation field from nearby massive hot stars, as we infer from a comparison of the recombination rate with the number of impinging Lyman continuum photons[3,13]. This conclusion is supported by the He I/Brγ line flux ratio of approximately 0.7, which is similar to the values found in the photo-ionized gas in the central parsec (0.35–0.7). If so, the requirement of complete photo-ionization sets a lower limit to f_V of $10^{-1 \pm 0.5}$ for the extreme case that the cloud is a thin sheet.

The combined astrometric and radial velocity data tightly constrain the cloud's motion. It is on a highly eccentric ($e = 0.94$) Keplerian orbit bound to the black hole (Fig. 1, Table 1 and Supplementary Information section 2). The pericentre radius is a mere 36 light hours (3,100 Schwarzschild radii, R_S), which the cloud will reach in summer 2013. Only the two stars S2 (r_{peri} = 17 light hours) and S14 (r_{peri} = 11 light hours) have come closer to the black hole[2,3] since our monitoring started in 1992. Although the cloud's gas density may be only modestly greater than that of other ionized gas clouds in the central parsec—$n_e \approx (0.1-2) \times 10^5$ cm^{-3}; refs 12 and 14—it has a specific angular momentum about 50 times smaller[12].

For the nominal properties of the X-ray detected accretion flow onto the black hole[15,16] the cloud should stay close to Keplerian motion all the way to the pericentre (Supplementary Information sections 3 and 4). Its density is currently about $300 f_V^{-1/2}$ times greater than that of the surrounding hot gas in the accretion flow[15]: extrapolating to the pericentre, its density contrast will then still be about $60 f_V^{-1/2}$. Similarly, the cloud's ram pressure by far exceeds that of the hot gas throughout the orbit. In contrast, the thermal pressure ratio will quickly decrease from unity at apocentre and the hot gas is expected to drive a shock slowly compressing the cloud. Whereas the external pressure compresses the cloud from all directions, the black hole's tidal forces shear the cloud along the direction of its motion, because the Roche density for self-gravitational stabilization exceeds the cloud density by nine orders of magnitude[3]. In addition, the ram pressure compresses the cloud parallel to its motion. The interaction between the fast-moving cloud and the surrounding hot gas should also lead to shredding and disruption, owing to the Kelvin–Helmholtz and Rayleigh–Taylor instabilities[17–20]. Rayleigh–Taylor instabilities at the leading edge should in fact break up the cloud within the next few years if it started as a spheroidal, thick blob (Supplementary Information section 3). A thin, dense sheet would by now already have fragmented and disintegrated, suggesting that f_V is of the order of unity.

We are witnessing the cloud's disruption happening in our spectroscopic data (Fig. 2). The intrinsic velocity width more than tripled over the last eight years, and we see between 2008 and 2011 a growing velocity gradient along the orbital direction. Test particle calculations implementing only the black hole's force show that an initially spherical gas cloud placed on the orbit (Table 1) is stretched along the orbit and compressed perpendicular to it, with increasing velocity widths and velocity gradients reasonably matching our observations (Fig. 3 and Supplementary Fig. 4). There is also a tail of gas with lower surface brightness on approximately the same orbit as the cloud, which cannot be due to tidal disruption alone. It may be stripped gas, or lower-density, lower-filling-factor gas on the same orbit. The latter explanation is more plausible given that the integrated Brγ and L′-band

[1]Max-Planck-Institut für extraterrestrische Physik (MPE), Giessenbachstrasse 1, D-85748 Garching, Germany. [2]Department of Physics, Le Conte Hall, University of California, Berkeley, California 94720, USA. [3]Department of Astronomy, University of California, Berkeley, California 94720, USA. [4]Universitätssternwarte der Ludwig-Maximilians-Universität, Scheinerstrasse 1, D-81679 München, Germany. [5]Departamento de Astronomía y Astrofísica, Pontificia Universidad Católica de Chile, Vicuña Mackenna 4860, 7820436 Macul, Santiago, Chile. [6]Center for Theoretical Astrophysics, Astronomy and Physics Departments, University of Illinois at Urbana-Champaign, 1002 West Green Street, Urbana, Illinois 61801, USA.

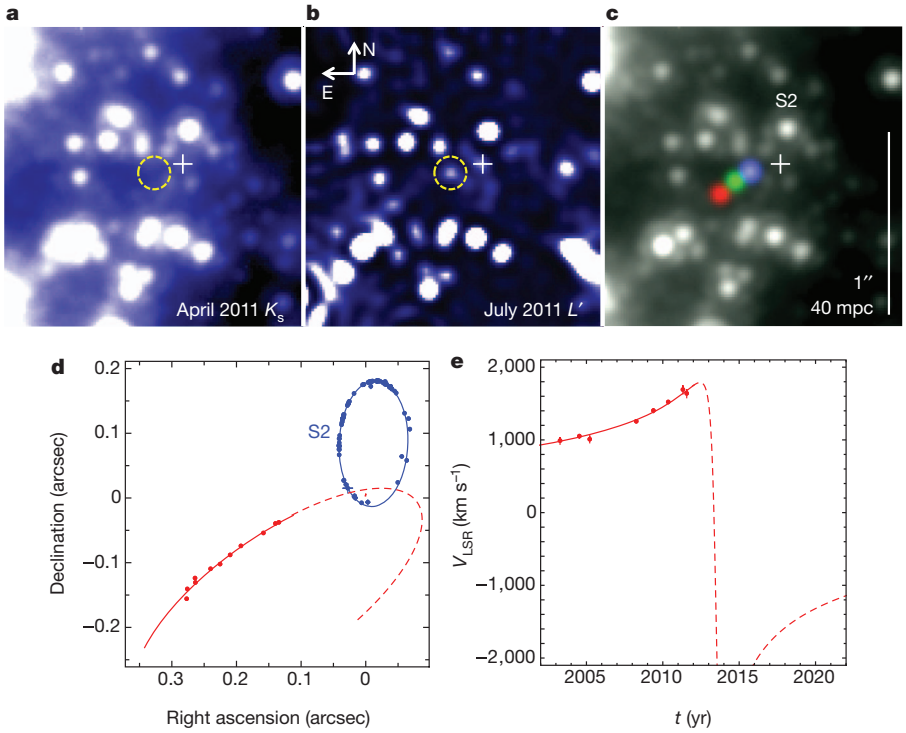

Figure 1 | Infalling dust/gas cloud in the Galactic Centre. **a**, **b**, NACO[9] adaptive optics VLT images showing that the cloud (dashed circle) is detected in the L′-band (3.76 μm, deconvolved and smoothed with a 2-pixel Gaussian kernel) but not in the K_s-band (2.16 μm, undeconvolved), indicating that it is not a star but a dusty cloud with a temperature of around 550 K (Supplementary Fig. 2). The cloud is also detected in the M-band (4.7 μm) but not seen in the H-band (1.65 μm). North is up, East is left. The white cross marks the position of Sgr A*. **c**, The proper motion derived from the L-band data is about 42 mas yr^{-1}, or 1,670 km s^{-1} (in 2011), from the southeast towards the position of Sgr A* (red for epoch 2004.5, green for 2008.3 and blue for 2011.3, overlaid on a 2011 K_s-band image). The cloud is also detected in deep spectroscopy with the adaptive-optics-assisted integral field unit SINFONI[10,11] in the H I $n = 7$–4 Brγ recombination line at 2.1661 μm and in He I at 2.058 μm, with a radial velocity of 1,250 km s^{-1} (in 2008) and 1,650 km s^{-1} (in 2011). **d**, **e**, The combination of the astrometric data in L′ and Brγ and the radial velocity (V_{LSR}) data in Brγ tightly constrains the orbit of the cloud (error bars are 1σ measurement errors). The cloud is on a highly eccentric, bound orbit ($e = 0.94$), with a pericentre radius and epoch of 36 light hours (3,100R_S) and 2013.5 (Table 1). The blue ellipse shows the orbit of the star S2 for comparison[1–3]. For further details see the Supplementary Information.

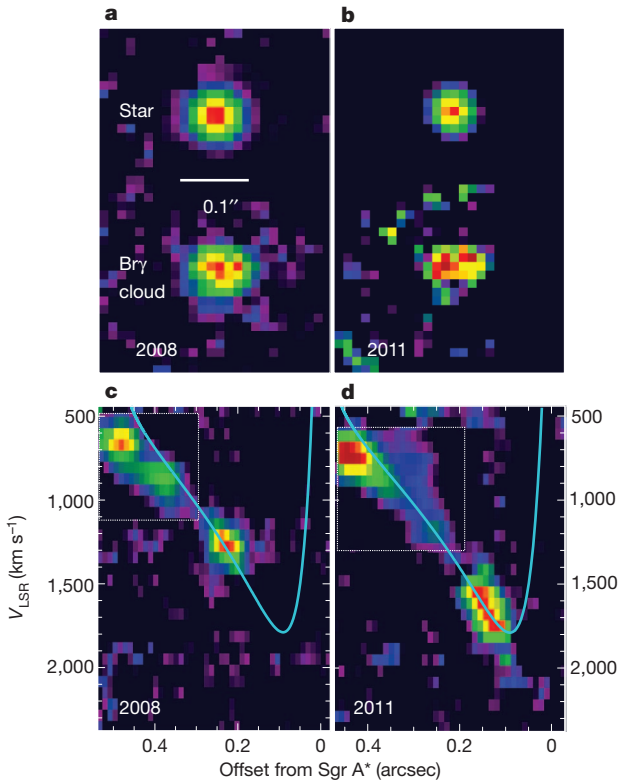

Figure 2 | The velocity shear in the gas cloud. The left column shows data from 2008.3, the right from 2011.3. Panels **a** and **b** show integrated Brγ maps of the cloud, in comparison to the point spread function from stellar images shown above. The inferred intrinsic East–West half-width at half-maximum source radii are $R_c = 21 \pm 5$ mas in 2008 and 19 ± 8 mas in 2011 (approximately along the direction of orbital motion), after removal of the instrumental broadening estimated from the stellar images above. A similar spatial extent is found from the spatial separation between the red- and blue-shifted emission of the cloud ($R_c = 23 \pm 5$ mas). The minor-axis radius of the cloud is only marginally resolved or unresolved (radius less than 12 mas). We adopt $R_c = 15$ mas as the 'effective' circular radius, by combining the results in the two directions. Panels **c** and **d** are position-velocity maps, obtained with SINFONI on the VLT, of the cloud's Brγ emission. The slit is oriented approximately along the long axis of the cloud and the projected orbital direction and has a width of 62 mas for the bright 'head' of the emission. For the lower-surface-brightness 'tail' of emission (in the enclosed white dotted regions) we smoothed the data with 50 mas and 138 km s^{-1} and used a slit width of 0.11″. The gas in the tail is spread over around 200 mas downstream of the cloud. The trailing emission appears to be connected by a smooth velocity gradient (of about 2 km s^{-1} mas^{-1}), and the velocity field in the tail approximately follows the best-fit orbit of the head (cyan curves; see also Table 1). An increasing velocity gradient has formed in the head between 2008 (2.1 km s^{-1} mas^{-1}) and 2011 (4.6 km s^{-1} mas^{-1}). As a result of this velocity gradient, the intrinsic integrated full-width at half-maximum (FWHM) velocity width of the cloud increased from 89 (±30) km s^{-1} in 2003 and 117 (±25) km s^{-1} in 2004, to 210 (±24) km s^{-1} in 2008, and 350 (±40) km s^{-1} in 2011.

Table 1 | Orbit parameters of the infalling cloud

Parameters of Keplerian orbit around the $4.31 \times 10^6 M_\odot$ black hole at $R_0 = 8.33$ kpc	Best-fitting value
Semi-major axis, a	521 ± 28 mas
Eccentricity, e	0.9384 ± 0.0066
Inclination of ascending node, i	106.55 ± 0.88 deg
Position angle of ascending node, Ω	101.5 ± 1.1 deg
Longitude of pericentre, ω	109.59 ± 0.78 deg
Time of pericentre, t_{peri}	2013.51 ± 0.035
Pericentre distance from black hole, r_{peri}	$4.0 \pm 0.3 \times 10^{15}$cm $= 3{,}140 R_S$
Orbital period, t_o	137 ± 11 years

luminosities did not drop by more than 30% between 2004 and 2011, and the integrated Brγ flux of the tail is comparable to that of the cloud.

The disruption and energy deposition processes in the next years until and after the pericentre passage are powerful probes of the physical conditions in the accretion zone (Supplementary section 3). We expect that the interaction between hot gas and cloud will drive a strong shock into the cloud. Given the densities of cloud and hot gas, the cloud as a whole should remain at low temperature until just before it reaches the pericentre. Near the pericentre the post-shock temperature of the cloud may increase rapidly to $T_{\mathrm{postshock,\,c}} \approx 6-10 \times 10^6$ K, resulting in X-ray emission. We estimate the observable 2−8-keV luminosity to be less than 10^{34} erg s^{-1} there, somewhat larger than the current 'quiescent' X-ray luminosity[6,15,21] of Sgr A* (10^{33} erg s^{-1}). Rayleigh–Taylor instabilities may by then have broken up the cloud into several fragments, in which case the emission may be variable throughout this period. Our predictions depend sensitively on the density and disruption state of the cloud, as well as on the radial dependencies of the hot gas properties, none of which we can fully quantify. The steeper the radial profiles are and the higher the value of f_V, the more X-ray emission will occur. Shallower profiles and a low value of f_V could shift the emission into the un-observable soft X-ray and ultraviolet bands. Together the evolution of the 2–8-keV and Brγ luminosities, as well as the Brγ velocity distribution, will strongly constrain the thermal states and interaction of the cloud and the ambient hot gas in the at present unprobed regime of $10^3 R_S - 10^4 R_S$, when compared with test particle calculations and more detailed numerical simulations (Fig. 3 and Supplementary Fig. 4).

The radiated energy estimated above is less than 1% of the total kinetic energy of the cloud, about $10^{45.4}$ erg. As the tidally disrupted filamentary cloud passes near pericentre some fraction of the gas may well collide with itself, dissipate and circularize[22]. This is probable because of the large velocity dispersion of the cloud, its size comparable to the impact parameter and because the Rayleigh–Taylor and Kelvin–Helmholtz timescales are similar to the orbital timescale. Because the mass of the cloud is larger than the mass of hot gas within the central $3{,}100 R_S$ or so (approximately $10^{27.3}$ g; ref. 15), it is plausible that then the accretion near the event horizon will be temporarily dominated by accretion of the cloud. This could in principle release up to around 10^{48} erg over the next decade, although the radiative efficiency of the inflow at these accretion rates is of the order of 1–10% (refs 23 and 24). Observations of the emission across the electromagnetic spectrum during this post-circularization phase will provide stringent constraints on the physics of black-hole accretion with unusually good knowledge of the mass available.

What was the origin of the low-angular-momentum cloud? Its orbital angular momentum vector is within 15° of the so-called 'clockwise' disk of young, massive O and Wolf–Rayet stars at radii of about 1″ to 10″ from Sgr A* (refs 3 and 25). Several of these stars have powerful winds. One star, IRS16SW, about 1.4″ southeast of Sgr A*, is a massive Wolf–Rayet contact binary[26]. Colliding winds in the stellar disk, and especially

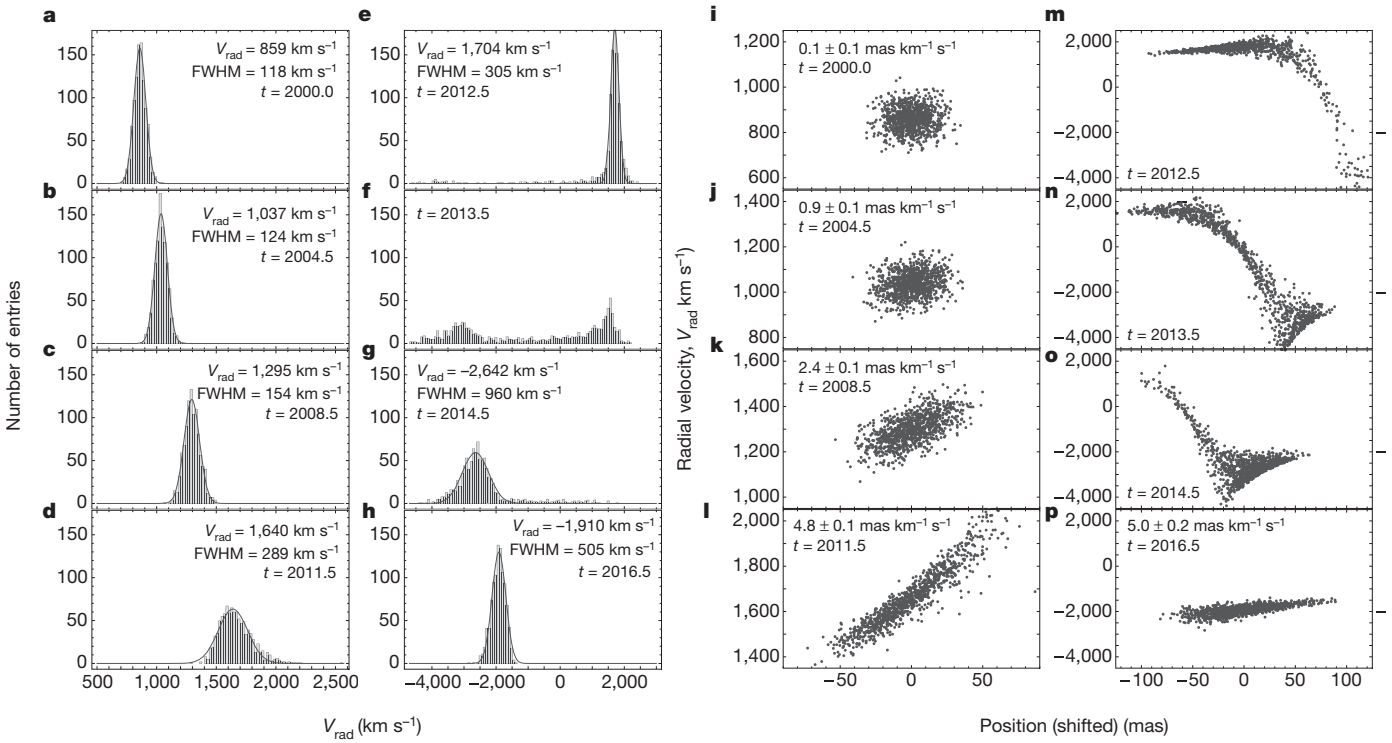

Figure 3 | Test particle simulation of the orbital tidal disruption. An initially Gaussian cloud of initial FWHM diameter 25 mas and FWHM velocity width 120 km s^{-1} is placed on the orbit in Table 1. **a**–**h**, As described in Supplementary Information section 4 (see also Supplementary Fig. 4) these panels show the evolution of the cloud integrated velocity width for eight epochs. The mean velocity and FWHM are given for those epochs at which the distribution is unimodal (that is, not **f**). **i**–**p**, These panels show the evolution of the velocity change as a function of position (measured in milli-arcseconds) along the orbital direction, purely on the basis of the tidal disruption of the cloud by the gravitational force of the supermassive black hole. This toy model is a good description of the velocity (and spatial) data between 2004 and 2011, thus allowing plausible forward projections until pericentre passage. Beyond that, the test particle approach will probably fail owing to the hydrodynamic effects, which will then most probably dominate further evolution. The cloud cannot be described by a simple velocity gradient between 2012 and 2015, and hence we omit the corresponding value in panels **m**, **n** and **o**.

in binaries, may create low-angular-momentum gas that then falls deep into the potential of the supermassive black hole[27,28].

Received 25 August; accepted 17 October 2011.
Published online 14 December 2011.

1. Ghez, A. M. *et al.* Measuring distance and properties of the Milky Way's central supermassive black hole with stellar orbits. *Astrophys. J.* **689,** 1044–1062 (2008).
2. Gillessen, S. *et al.* Monitoring stellar orbits around the massive black hole in the Galactic Center. *Astrophys. J.* **692,** 1075–1109 (2009).
3. Genzel, R., Eisenhauer, F. & Gillessen, S. The Galactic Center massive black hole and nuclear star cluster. *Rev. Mod. Phys.* **82,** 3121–3195 (2010).
4. Reid, M. J., Menten, K. M., Trippe, S., Ott, T. & Genzel, R. The position of Sagittarius A*. III. Motion of the stellar cusp. *Astrophys. J.* **659,** 378–388 (2007).
5. Doeleman, S. S. *et al.* Event-horizon-scale structure in the supermassive black hole candidate at the Galactic Centre. *Nature* **455,** 78–80 (2008).
6. Baganoff, F. K. *et al.* Rapid X-ray flaring from the direction of the supermassive black hole at the Galactic Centre. *Nature* **413,** 45–48 (2001).
7. Genzel, R. *et al.* Near-infrared flares from accreting gas around the supermassive black hole at the Galactic Centre. *Nature* **425,** 934–937 (2003).
8. Marrone, D. P., Moran, J. M., Zhao, J.-H. & Rao, R. An unambiguous detection of Faraday rotation in Sagittarius A*. *Astrophys. J.* **654,** L57–L60 (2007).
9. Lenzen, R., Hofmann, R., Bizenberger, P. & Tusche, A. CONICA: the high-resolution near-infrared camera for the ESO VLT. *Proc. SPIE* (ed. Fowler, A. M.) **3354,** 606–614 (1998).
10. Eisenhauer, F. *et al.* SINFONI—Integral field spectroscopy at 50 milli-arcsecond resolution with the ESO VLT. *Proc. SPIE* (eds Iye, M. & Moorwood, A. F. M.) **4841,** 1548–1561 (2003).
11. Bonnet, H. *et al.* Implementation of MACAO for SINFONI at the Cassegrain focus of VLT, in NGS and LGS modes. *Proc. SPIE* (ed. Wizinowich, P.) **4839,** 329–343 (2003).
12. Zhao, J. H., Morris, M. M., Goss, W. M. & An, T. Dynamics of ionized gas at the Galactic Center: Very Large Array observations of the three-dimensional velocity field and location of the ionized streams in Sagittarius A West. *Astrophys. J.* **699,** 186–214 (2009).
13. Martins, F. *et al.* Stellar and wind properties of massive stars in the central parsec of the Galaxy. *Astron. Astrophys.* **468,** 233–254 (2007).
14. Scoville, N. Z., Stolovy, S. R., Rieke, M., Christopher, M. & Yusef-Zadeh, F. Hubble Space Telescope Paα and 1.9 micron imaging of Sagittarius A West. *Astrophys. J.* **594,** 294–311 (2003).
15. Xu, Y.-D., Narayan, R., Quataert, E., Yuan, F. & Baganoff, F. K. Thermal X-ray iron line emission from the Galactic Center black hole Sagittarius A*. *Astrophys. J.* **640,** 319–326 (2006).
16. Yuan, F., Quataert, E. & Narajan, R. Nonthermal electrons in radiatively inefficient accretion flow models of Sagittarius A*. *Astrophys. J.* **598,** 301–312 (2003).
17. Klein, R. I., McKee, C. F. & Colella, P. On the hydrodynamic interaction of shock waves with interstellar clouds. 1: Nonradiative shocks in small clouds. *Astrophys. J.* **420,** 213–236 (1994).
18. Chandrasekhar, S. *Hydrodynamic and Hydromagnetic Stability* 428–514 (Dover Publications, 1961).
19. Murray, S. D., &. Lin, D. N. C. Energy dissipation in multiphase infalling clouds in galaxy halos. *Astrophys. J.* **615,** 586–594 (2004).
20. Cooper, J. L., Bicknell, G. V., Sutherland, R. S. & Bland-Hawthorn, J. Starburst-driven galactic winds: filament formation and emission processes. *Astrophys. J.* **703,** 330–347 (2009).
21. Baganoff, F. K. *et al.* Chandra X-ray spectroscopic imaging of Sgr A* and the central parsec of the Galaxy. *Astrophys. J.* **591,** 891–915 (2003).
22. Sanders, R. H. The circumnuclear material in the Galactic Centre—a clue to the accretion process. *Mon. Not. R. Astron. Soc.* **294,** 35–46 (1998).
23. Sharma, P. Quataert, E. Hammett, G. W. & Stone, J. M. Electron heating in hot accretion flows. *Astrophys. J.* **667,** 714–723 (2007).
24. Blandford, R. D. & Begelman, M. C. On the fate of gas accreting at a low rate on to a black hole. *Mon. Not. R. Astron. Soc.* **303,** L1–L5 (1999).
25. Bartko, H. *et al.* Evidence for warped disks of young stars in the Galactic Center. *Astrophys. J.* **697,** 1741–1763 (2009).
26. Martins, F. *et al.* GCIRS 16SW: a massive eclipsing binary in the Galactic Center. *Astrophys. J.* **649,** L103–L106 (2006).
27. Ozernoy, L. M., Genzel, R. & Usov, V. V. Colliding winds in the stellar core at the Galactic Centre: some implications. *Mon. Not. R. Astron. Soc.* **288,** 237–244 (1997).
28. Cuadra, J., Nayakshin, S., Springel, V. & Di Matteo, T. Accretion of cool stellar winds on to Sgr A*: another puzzle of the Galactic Centre? *Mon. Not. R. Astron. Soc.* **260,** L55–L59 (2005).

Supplementary Information is linked to the online version of the paper at www.nature.com/nature.

Acknowledgements This paper is based on observations at the Very Large Telescope (VLT) of the European Observatory (ESO) in Chile. We thank C. McKee and R. Klein for discussions on the cloud destruction process. J.C. acknowledges support from FONDAP, FONDECYT, Basal and VRI-PUC. A.B. acknowledges the support of the excellence cluster 'Origin and Structure of the Universe'.

Author Contributions S.G. collected and analysed the data and discovered the orbit of the gas cloud. R.G. and S.G. wrote the paper. T.K.F. detected the high proper motion and extracted the astrometric positions and the photometry. R.G., A.B. and E.Q. derived the cloud's properties, its evolution and the estimate of the X-ray luminosity. R.G., E.Q., A.B. and C.F.G. contributed to the analytical estimates. C.A. and J.C. set up numerical simulations to check the analysis. F.E., O.P. and K.D.-E. helped in the data analysis and interpretation. T.O. provided valuable software tools.

Author Information Reprints and permissions information is available at www.nature.com/reprints. The authors declare no competing financial interests. Readers are welcome to comment on the online version of this article at www.nature.com/nature. Correspondence and requests for materials should be addressed to S.G. (ste@mpe.mpg.de) or R.G. (genzel@mpe.mpg.de).